UDK621.3:(53+54+621+66), ISSN0352-9045 Informacije MIDEM 33(2003)1, Ljubljana

ELECTRIC FIELD AND POTENTIAL AROUND IMPURITY ATOMS IN SEMICONDUCTORS

Andrej Levstek, Jože Furlan

University of Ljubljana, Faculty of electrical engineering, Ljubljana, Slovenia

Key words: physics, electronics, electrostatics, semiconductor modeling, Coulomb potential, microscopic electric potential, microscopic electric field intensity, Debye-Hückel screening, analytical approximation, numerical solution

Abstract: The paper describes different models for the microscopic electric field intensity and electric potential in the surroundings of ionized impurity atoms in semiconductors. The emphasis is placed on a novel comprehensive model that is an improvement of the Debye-Hückel screening applied to semiconductors. In contrast to other described models, the improved model is featured by respecting all three mechanisms of electric field attenuation in solids: dielectric polarization, free carrier screening, and spatial distribution of impurity atoms. Electric potential and electric field intensity profiles are obtained as numerical solutions of the Poisson equation fully respecting the non-linear space charge dependency. Proposed analytical approximations of numerical results facilitate their further use.

Električno polje in potencial v okolici atomov primesi v polprevodnikih

Ključne besede: fizika, elektronika, elektrostatika, modeliranje polprevodnikov, Coulombov potencial, mikroskopski električni potencial, mikroskopska električna poljska jakost, Debye-Hücklov model zakrivanja, analitična aproksimacija, numerična rešitev

Izvleček: V prispevku so opisani različni modeli mikroskopskega električnega polja in potenciala v okolici ioniziranih atomov primesi v polprevodnikih. Poseben poudarek je posvečen novemu izčrpnemu modelu, ki predstavlja izboljšavo uporabe Debye-Hücklovega modela zakritega polja v polprevodnikih. Za razliko od ostalih opisanih modelov, se izboljšana inačica odlikuje s tem, da so upoštevani vsi trije mehanizmi slabljenja električnega polja v trdnih snoveh: dielektrična polarizacija, zakrivanje polja s prostimi nosilci in vpliv sosednjih, prostorsko razporejenih, ioniziranih atomov primesi. Poteki električnega polja in potenciala so izračunani z numeričnim reševanjem Poissonove enačbe z upoštevanjem nelinearne odvisnosti prostorskega naboja. Dobljeni numerični poteki so aproksimirani z analitičnimi funkcijami, ki olajšajo njihovo nadaljnjo uporabo.

1 Introduction

Properties of various semiconductor devices are usually described by analytical approaches based on the macroscopic model of the semiconductor structure. In such models uniform microscopic structure is presumed, e.g., the edge of the conducting band varies only macroscopically because of the built-in impurity concentration profile. Analytical approaches are usually applied only to one-dimensional semiconductor structures. Two or even three-dimensional analyses are prevalently carried out numerically as in many cases analytical solutions are not feasible.

For analysis, description and understanding of certain phenomena it is inevitably necessary to consider local variations of microscopic space charge, electric field and potential. Scattering and capture of free charge carriers by localized charges consisting of ionized impurities represent an important type of such phenomena. Microscopic gradients of the electric potential play also an important role at the increase of the concentration of thermally emitted free carriers from the energy states within the gap across the lowered potential barrier into the conduction or valence band (Poole-Frenkel effect), tunneling of charge carriers through thin potential barriers, etc.

The microscopic electric potential in the surroundings of an ionized impurity atom is affected by three main factors, namely, the atoms of the base semiconductor, mobile charge carriers, and adjacent ionized impurities. Each of these factors weakens the electric field strength and electric potential in its own way. The most accurate result is obtained when all factors are taken into account. Of course, this is not an easy task especially if analytical expressions for the electric potential are desired. However, it is possible to find approximate analytical expressions if some effects are simplified or neglected.

In order to maintain the main ideas clear we will constrain this discussion to n-type semiconductor that is easier to describe and understand. Majority mobile charge carriers in n-type are electrons hence the physical picture is less demanding, as electrons are real particles. Further, all numerical examples and presented diagrams are calculated for silicon since it is the most important semiconductor material.

From the beginning to the end of this article, we shall increase the degree of complexity involved with the described solutions of the microscopic electric potential.

2 Coulomb potential

Silicon crystalline structure is tetrahedral, i.e. each silicon atom is tied to its four neighbors by covalent bonds consisting of a common pair of valence electrons. In n-type silicon, a small part of Si atoms is replaced by donors, i.e., impurity atoms with five valence electrons. Four valence electrons form covalent bonds to the four neighboring silicon atoms leaving the fifth one loosely tied to the core. The space around impurities is filled with host atoms Si that weaken the electrostatic force in such an extent that at room temperature almost all donors are ionized /1/. In other words, the fifth electron of almost every donor atom gets sufficient kinetic energy to become mobile. Impurity atoms themselves remain firmly bound to the host lattice and can be treated as a uniform spatial distribution fixed-point charges $+q$. However, the spatial pattern of impurities is not a strict arrangement in the sense of a crystal lattice, but it is uniform on the average with minor deviations from its regular positions. The process of ionization does not change the neutrality of the observed volume on the macroscopic level, because the interstitial space is filed with mobile electrons, which contribute the negative charge that exactly compensates the positive charge of fixed ions.

2.1 Electric potential of an isolated ion

The straightforward solution of the electric potential of an ionized impurity atom can be derived from Coulomb's law /2/ since an ionized impurity can be viewed as an isolated point charge $+q$

$$V(r) = \frac{q}{4\pi\varepsilon r}, \quad (1)$$

where q denotes the elementary charge, r is the distance from the point charge and ε is the dielectric constant (permittivity) of the environment. Eq. is well known as Coulomb potential. The potential at a certain point in space is meaningful only when a reference zero-potential point is specified. In most cases, this point is taken at infinity.

The electrostatic potential of an ionized impurity atom alters the shape of band-edge potentials in the close surroundings. The resulting joint profile is obtained by simple scalar addition of the potentials. This is a significant advantage of using electric potential V rather than electric field intensity **E**. The diagram of band-edge potentials, shown in Fig. 1, illustrates the influence of the Coulomb potential of an ionized donor in silicon.

The diagram in Fig. 1 is only one-dimensional representation of the spherically symmetric spatial field. It is actually the plot of the potential along a straight line, which is laid through the charged center. The valence and conducting band-edge potential are denoted by V_V and V_C, respectively. With increasing distance r, those potentials asymptotically approach their macroscopic values V_{V0} and V_{C0}.

In the described Coulomb potential model, only dielectric attenuation is taken into account. Dielectric polarization of

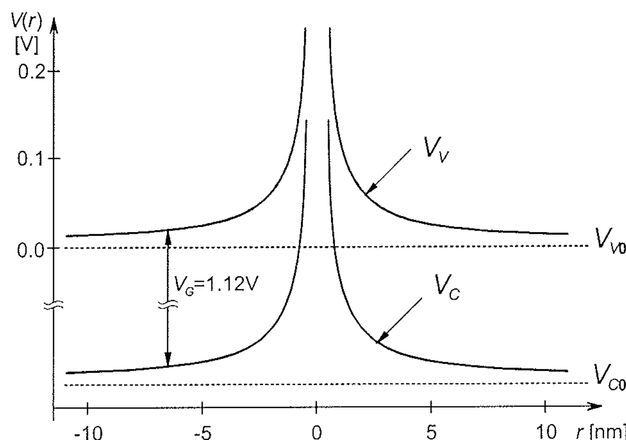

Fig. 1: Band-edge potentials in silicon modified by the Coulomb potential of an isolated ionized donor atom at r = *0.*

host semiconductor atoms is responsible for the reduction of the electric field. The application of the macroscopic dielectric constant for microscopic fields /1/, /3/ is justified by the fact that the distance between host atoms is much smaller, e.g., 0.235 nm for silicon, than the distances of interest.

Permittivities of materials are usually expressed as a product of the permittivity of empty space ε_0 and the relative permittivity ε_r of a particular material. For common semiconductor materials ε_r ranges approx. from 9 to 17, in particular for silicon we get ε_r = 11.7 /4/. These relatively high values of ε_r reduce the electric potential and the associated binding energy of donors after being incorporated in host semiconductor.

Finally, the term *isolated impurity* needs some explanation. We use this expression for semiconductor doped with very low concentrations, which result in a sparse spatial distribution of impurities, such that the mutual influences between immediate neighbors are diminished by large average distances to a negligible level. There is no explicit margin of the doping N_D, below which the impurities are considered isolated, but as a rule of thumb $N_D = 10^{14}$ cm^{-3} can be used for silicon.

2.2 Effect of neighbors

Practical doping concentrations are substantially higher than 10^{14} cm^{-3} therefore, influences of the ionized impurity atoms in the neighborhood have to be taken into account. Neighbors modify the potential and electric field distribution of an isolated ion (1), introducing saddles between adjacent charged centers /5/. The modified circumstances can be easily explained by the rough draft of the electrical potential profile along the straight-line laid through two adjoining charged centers shown in Fig. 2.

The joint potential is obtained by adding the Coulomb potentials (1) of each ionized atom, one at the origin and the other at $r = 2R$. For distances $0 < r < 2R$ we get

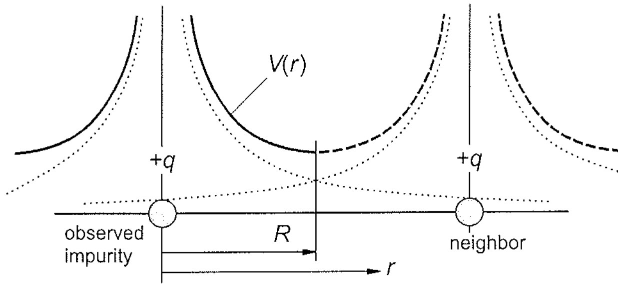

Fig. 2: Schematic representation of the electric potential along the straight-line running through two adjoining ionized impurity atoms in n-type semiconductor.

$$V(r) = \frac{q}{4\pi\varepsilon r} + \frac{q}{4\pi\varepsilon(2R-r)}. \quad (2)$$

Adjacent impurity atoms are brought closer to each other as their concentration N_D increases regardless of their spatial distribution. Consequently, an increased impurity concentration raises the potential saddle at $r = R$. The diagram shown in Fig. 2 is valid also for other directions in space where other neighbors are positioned. If impurities are assumed to have a simple body-centered cubic lattice then each ion is surrounded with six closest neighbors. Though the ideal spherical symmetry of the isolated ion potential is perturbed, high degree of central symmetry remains for radii $r \leq R$ where Eq. (2) may be applied in any direction. It is important to note that the magnitude of the electric field intensity E drops to zero at $r = R$ where the potential has a local minimum. At this stage, we will not discuss the exact diagram of band-edge potentials because in this case the zero-valued reference point at infinity does not exist. The modified band structure will be presented in section 4.1.

3 Debye-Hückel screened potential

Free carriers, which are randomly moving in the space between the ionized impurities, compensate the space charge of fixed ions. The electrostatic field is screened by mobile carriers due to electric forces that concentrate the cloud of charge carriers near ionized impurity atoms. Such phenomena have been noticed and first addressed in the context of electrolytes by Debye and Hückel /6/. This model can be applied to analyze the screened Coulomb potential of one ionized impurity atom. One has to be aware that the Debye-Hückel (DH) theory of screening is based upon simplifications, which are justified for dilute ionic solutions, in order to obtain an analytical expression for the screened potential. Thus, the DH model involves some deficiencies, which become rather important when this model is applied to semiconductors.

The expression for the screened potential is derived by solving Poisson's equation /1/,/7/

$$\nabla^2 V = -\frac{\rho}{\varepsilon}, \quad (3)$$

where e is the macroscopic permittivity of the host semiconductor and ρ is the space charge consisting of rigid ionized impurities and mobile carries. For n-type semiconductor the charges of ionized impurity atoms and free electrons mutually cancel each other. Only the charge of one electron remains, since the positive charge of the observed ion is left out. The solution of (3) is obtained by the linearized Boltzmann distribution that is used for $\rho(V)$.

For an n-type semiconductor with impurity concentration N_D the DH screened Coulomb potential around the fixed ionized impurity atom is expressed by /8/

$$V(r) = \frac{q}{4\pi\varepsilon r}\exp\left(-\frac{r}{L_D}\right), \quad (4)$$

where L_D is *Debye length,* given by

$$L_D = \sqrt{\frac{kT\varepsilon}{q^2 N_D}}. \quad (5)$$

Two important distinctions should be made between the circumstances in semiconductors and those in electrolytic solutions, on which the DH model is focused:

i. Ions are rigidly built in the crystal structure of the semiconductor
ii. Mobile carries are unipolar (of only one polarity) as long as the observed semiconductor is not intrinsic, i.e., N_D is at least an order of magnitude bigger than n_i.

The DH screened potential has zero-valued reference point at infinity hence it can be easily compared with the Coulomb potential V_{Cou}. Plots of both potentials vs. distance r for silicon ($N_D = 10^{17}$ cm^{-3}) are shown diagram in Fig. 3.

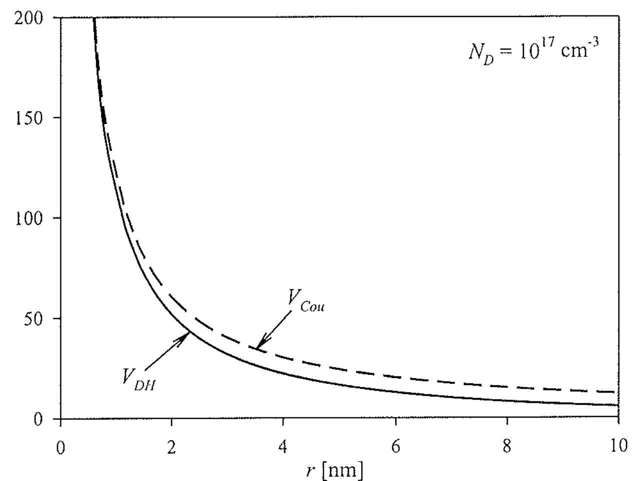

Fig. 3: Microscopic potential against distance r from ionized impurity in Si.
(¦¦): screened DH potential Eq. (3)
(—): unscreened Coulomb potential Eq. (1)

The plot of DH screened potential V_{DH} declines steeper and is always lower than the Coulomb potential. The degree of reduction is governed by the exponential factor in Eq. (4) that depends on impurity concentration N_D. The DH approach does not include the influence of neighboring ions that significantly modify the shape of the potential as it is shown in section 3.2.

4 Comprehensive model of the microscopic potential

4.1 Numerical solution

The exact screened potential, which respects the above-mentioned effects at the highest possible extent, can be calculated only numerically. In this section, we will present only the important starting assumptions and the main steps of the method. More details can be found in /9/, /10/.

Unlike the Debye-Hückel approach, which examines the potential of a single ion within an unlimited space, the combined approach is focused on a finite volume confined by the same volumes placed around the neighboring fixed ions. The volume is approximated with a sphere whose diameter is equal to the closest distance between adjoining ions. This approximation substantially simplifies the mathematical complexity of the problem, as the electric potential field possesses spherical symmetry. As it is shown in section 2.2, the potential $V(r)$ becomes flat at midway between adjacent impurities

$$\left.\frac{dV}{dr}\right|_{r=R} = 0 \tag{6}$$

The microscopic potential is obtained by solving the Poisson differential equation (3) for boundary condition (6). In spherical coordinates, Eq. (3) becomes an ordinary differential equation

$$\frac{d^2V}{dr^2} + \frac{2}{r}\frac{dV}{dr} = -\frac{\rho}{\varepsilon}, \tag{7}$$

as central symmetry of the potential and space charge is presumed. Space charge density ρ of the electron cloud is expressed by electron concentration $n(r)$ that is determined by the density of states distribution in the conduction band and by Fermi-Dirac occupation probability, defining

$$\rho = -qn = -qN_c F_{1/2}(\eta_C), \tag{8}$$

where N_c is the effective conduction band density of states and $F_{1/2}(\eta_c)$ is the Fermi-Dirac integral, which is approximated by analytical functions in various regions of normalized potential $\eta_c = q(V_F - V_C)/kT$ /11/.

The screened potential of the localized charge V, which modifies V_C and thus the space charge density ρ (8), has to meet the neutrality condition that can be expressed in integral form

$$\iiint_{V_S} \rho\, dv + q = 0, \tag{9}$$

where V_S denotes the observed sphere. The a priori unknown difference $V_R = V_C - V_{C0}$ at midway $r = R$, upon which the total charge of the electron cloud depends, is determined by an iterative algorithm. The non-linear Poisson equation, obtained by inserting (8) into (7), is solved by numerical integration, which starts at midway $r = R$, using boundary condition (6) and an initial guess value V_R. After each iteration, V_R is successively adjusted until the neutrality condition (9) is achieved.

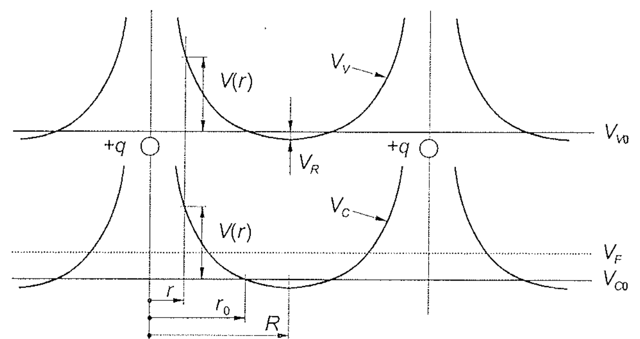

Fig. 4: Schematic diagram of band-edge potentials on a straight line running through two positive ions. Macroscopic band-edge potentials V_{V0} and V_{C0} are modified by the screened potential V(r).

The band-edge potentials are then given by

$$V_C = V_{C0} + V, \tag{10}$$

and similarly

$$V_V = V_{V0} + V. \tag{11}$$

Schematic diagram of screened band-edge potentials is shown in Fig. 4, where some important properties of the final solution can be seen. The polarity of V is both, positive and negative, thus conduction band-edge potential V_C is located partly above and partly below its macroscopic value V_{C0}. This variation of V_C is accompanied with similar but more intense deviations of the electron density n from its macroscopic equilibrium value N_D. In the spherical region close to the ion, the concentration of free electrons n is much above N_D. This increased negative space charge is compensated by $n < N_D$ in the outer shell in order to meet the neutrality condition (9). The screened potential V is always negative for radii r beyond a certain $r > r_0$ (see Fig. 4), hence $V_R = V(R)$ is always slightly negative.

The range of the horizontal axis in Fig. 5 covers all the radii within the observed sphere from 0 to R, because for simple cubic spatial distribution of impurities and $N_D = 10^{17}\text{cm}^{-3}$, we get $R = 10^{-8}$ m.

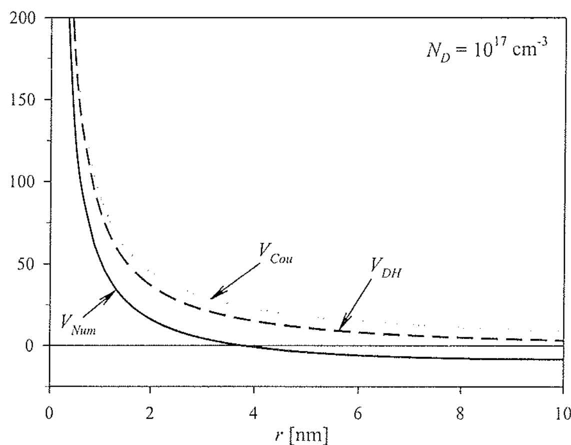

Fig. 5: Numerical and classical potentials against distance r from ionized impurity in n-type Si, $N_D = 10^{17} cm^{-3}$.
(¦¦): screened potential - numerical solution of Eq. (7)
(—): screened DH potential Eq. (3)
(·····): unscreened Coulomb potential Eq. (1)

The numerically computed potential, combines all three major mechanisms that attenuate the electric potential as we move from the charged center, i.e., dielectric polarization, space charge screening, and the influence of adjacent ions, thus it exhibits a significant improvement upon the classical expressions, i.e., the Coulomb and DH potential, respectively.

4.2 Analytical approximations

4.2.1 Screened electric field intensity

The main drawbacks of the numerical method are, first, the very nature of numerical results, which are usually obtained in tabular form, and second, the extensive and time-consuming iterative algorithm. In this section, we present analytical approximations proposed in /10/ for the numerical solution of the microscopic electric field and potential, respectively. Throughout this article, the main emphasis is put on the electric potential, owing to its scalar nature and its tight connection to energy bands in semiconductor. Though in some cases, especially those involved with kinematics of charged particles, electric field intensity **E** seems to be more appropriate.

The magnitude of electric field intensity E of a positive charge q given by Coulomb's law

$$E = \frac{q}{4\pi\varepsilon r^2}, \qquad (12)$$

becomes zero only when the distance r gets infinite. The same applies to DH screened electric field, which is obtained by differentiating the potential (4). The boundary condition (6), which is postulated to mimic the effect of neighbors, can be met by an approximate expression for the electric field in the range $0 < r < R$ in the form

$$E = \frac{q}{4\pi\varepsilon r^2}\left[1-\left(\frac{r}{R}\right)^m\right] \qquad (13)$$

in which the screening effect is contained in the factor $[1 - (r/R)^m]$, where m determines the degree of screening. The general Eq. (13) satisfies the boundary condition (6) for any selected value of m. When lowering the exponent m, the electric field decreases more vigorously with an increasing radius r, thus enhancing the screening effect. At low values of r/R the electric field in Eq. (13) approaches the unscreened Coulomb case.

The optimal value m_{opt}, which minimizes the total squared error between the analytic approximation and the numerical solution, is shown /10/ to depend slightly on the impurity concentration. The exponent m_{opt} decreases from 1.8 to 0.9 as the impurity concentration N_D is being increased from 10^{15} up to 10^{19} cm^{-3}, respectively. If simplicity of the analytical expression is desired then integer values 1 and 2 are preferred.

The diagram in Fig. 6 shows different plots of the magnitude of electric field intensity in the surroundings of an ionized impurity atom, namely, E_{Cou} given by (12) (Coulomb's law), E_{Num} is obtained numerically, using the algorithm presented in previous section, and E_{App} according to the analytical approximation with $m = 1.5$. The plot of the approximate electric field E_{App} exhibits very good matching to the numerical electric field E_{Num}, which is considered accurate. The values of E_{Num} and V_{Num} are computed simultaneously when the Poisson's equation (7) is being solved.

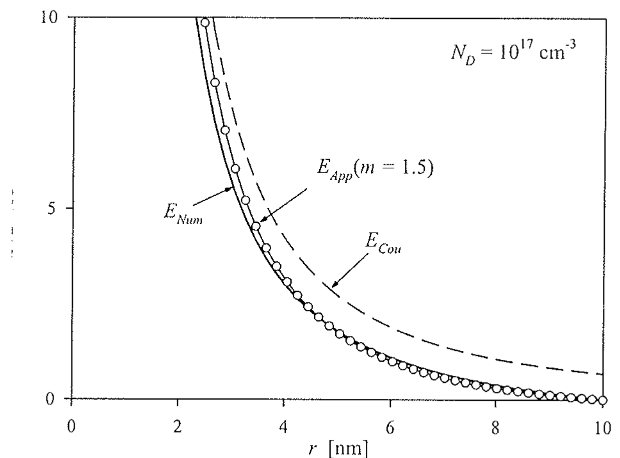

Fig. 6: Magnitude of electric field intensity in the region of an ionized impurity atom in n-type Si, $N_D = 10^{17} cm^{-3}$.
(——): numerical solution
(oooo): analytical approximation Eq. (13) with m = 1.5
(- - - -): unscreened Coulomb electric field Eq. (12)

4.2.2 Screened electric potential

In order to analyze the effect of the proposed approximation (13), an electrostatic potential for arbitrary m is ob-

tained. Integrating Eq. (13) in the range from R to arbitrary r gives the form

$$V - V_R = \frac{q}{4\pi\varepsilon r}\left[1 + \frac{1}{(m-1)}\left(\frac{r}{R}\right)^m - \frac{m}{(m-1)}\frac{r}{R}\right], \quad (4)$$

where V_R is the potential at $r = R$, referenced to the macroscopic band-edge potential V_{C0} (see Fig. 4). The expression is valid even for $m = 1$ since the limit $\lim_{m\to 1}(V - V_R)$ exists. In this special case Eq. (14) changes to

$$V - V_R = \frac{q}{4\pi\varepsilon r}\left(1 - \frac{r}{R} + \frac{r}{R}\ln\frac{r}{R}\right). \quad (15)$$

The exact value of V_R can be obtained numerically from the boundary condition (9) and Eq. (8) for the space charge of the electron cloud. However, it is possible to obtain an approximate value of V_R by expressing the electron concentration with the Boltzmann instead of the Fermi-Dirac distribution. The derivation of V_R /10/ yields two final analytical expressions for the screened potential:

$$V = \frac{q}{4\pi\varepsilon r}\left[1 + \frac{1}{(m-1)}\left(\frac{r}{R}\right)^m - \frac{3}{2}\frac{m(m+1)}{(m-1)(m+2)}\frac{r}{R}\right], \quad (16)$$

for the general value of $m \neq 1$ and

$$V = \frac{q}{4\pi\varepsilon r}\left[1 + \ln\frac{r}{R}\left(\frac{r}{R}\right) - \frac{7}{6}\frac{r}{R}\right], \quad (17)$$

for the special case with $m = 1$.

An evaluation of the approximate screened potential (16) is shown in Fig. 7. The approximation V_{App} with $m = 1.5$ is plotted together with the numerical potential V_{Num} discussed in section 4.1 and Coulomb potential V_{Cou}, which is shown for reference. The value of the exponent m is not exactly the optimal value for $N_D = 10^{17}\text{cm}^{-3}$, but is a reasonable choice for most doping concentrations that appear in electron devices.

The shapes of the potential profiles V_{App} and V_{Num} are in good agreement over the whole range of distances. However, there is small constant difference between the two potentials that are being compared. In contrast with the interweaving plots of electric field E_{App} and E_{Num} in Fig. 6, the potential V_{App} remains slightly above V_{Num} over the entire range of radii. This difference arises from the derivation of V_R, in which linearization of the Boltzmann exponential dependency is used.

5 Conclusion

The intention of this article was to present a review of the various models for the microscopic electric field and potential. The described models were devised or modified

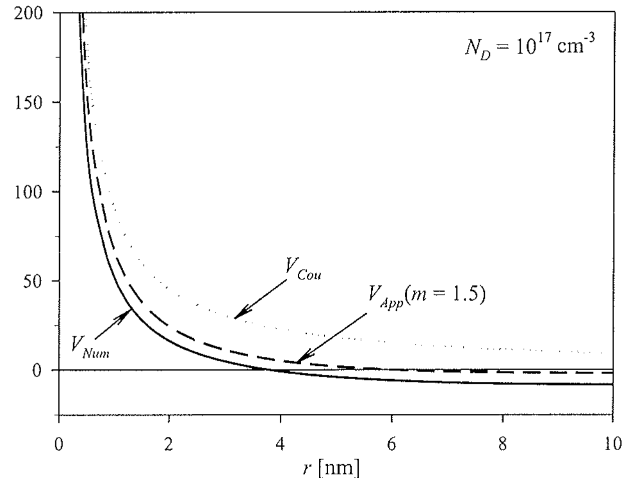

Fig. 7: Approximate and numerical potential versus distance r from ionized impurity in n-type Si, $N_D = 10^{17}\text{cm}^{-3}$.
(——): screened potential V_{Num} - numerical solution of Eq. (7)
(- - -): analytical approximation V_{App} Eq. (16) with m = 1.5
(·····): unscreened Coulomb potential Eq. (1)

for the use in semiconductors, however, some of them, e.g. the numerical method, can be applied also in other areas.

In order to maintain informational nature and clearness of the paper many details and results have been omitted. Extensive tests of numerical method for the whole range of interesting doping concentrations have been carried out. The results show god agreement between the approximate and numerical profiles.

Numerically calculated potential and its approximation represent a significant improvement of the DH model, because all three mechanisms of electric field attenuation (dielectric polarization, screening by mobile charge carriers, effects of neighbor impurity atoms) are taken into account. The choice of the appropriate model in a particular case depends on a variety of factors. As general rule, it can be suggested that in cases where higher doping concentrations are concerned a comprehensive model would be more appropriate, since the effect of screening is more intense at high space charge densities.

6 References

/1/ C. T. Sah, *Fundamentals of Solid-State Electronics,* World Scientific Publishing Co., Singapore, 1991

/2/ D. K. Cheng, *Field and Wave Electromagnetics*, Addison-Wesley Publishing Company, Reading 1989

/3/ W. Shockley, *Electrons and Holes in Semiconductors*, D. Van Nostrand Co., New York 1951

/4/ M. E. Levinshtein, S.L. Rumyantsev, *Handbook Series on Semiconductor Parameters*, vol.1, M. Levinshtein, S. Rumyantsev and M. Shur, ed., World Scientific, London, 1996

/5/ K. W. Böer, "The Conduction Mechanism of Highly Disordered Semiconductors II. Influence of Charged Defects", *phys. stat. sol.*, vol. 84, pp. 733-740, 1969

/6/ J.O'M. Bockris, A. K. N. Reddy, *Modern Electrochemistry, Vol 1*, Pllenum Press, New York 1970

/7/ W. J. Moore, *Physical Chemistry*, Addison Wesley Longman, London 1972

/8/ K. W. Böer, *Survey of Semiconductor Physics*, Van Nostrand Reinhold, New York 1990

/9/ A. Levstek, J. Furlan: Approaches to the theory of microscopic potential and free carrier distribution in semiconductor, Proc. 36th Int. Conf. on Microelectronics, Devices and Materials and the Workshop on Analytical Methods in Microelectronics and Electronic Materials, October 18 - 20, 2000, Postojna, Slovenia, pp. 329-334.

/10/ A. Levstek, J. Furlan, "Microscopic electric field in the surroundings of ionized impurities in semiconductor", *Journal of Electrostatics*, (in press)

/11/ J. S. Blackmore, Approximations for Fermi-Dirac Integrals. Especially the Function $F_{1/2}(h)$ Used to describe Electron Density in a Semiconductor, Solid-St Electron, 25, (1982), 1067-1076.

mag. Andrej Levstek
dr. Jože Furlan
University of Ljubljana
Faculty of Electrical Engineering
Tržaška c. 25, 1000 Ljubljana, Slovenia
Tel.: +386 1 4768 325, Fax: +386 1 4264 630
Email: andrej.levstek@fe.uni-lj.si

Prispelo (Arrived): 29.07.2002 Sprejeto (Accepted): 25.03.2003